AD-A157 454 DEVELOPMENT OF A NAVIER-STOKES ANALYSIS FOR THE FLOW IN 1/1
DISK PUMPS..(U) SCIENTIFIC RESEARCH ASSOCIATES INC
GLASTONBURY CT Y N KIM ET AL. APR 85 SRA-910008F
UNCLASSIFIED AFWAL-TR-85-2039 F33615-84-C-2469 F/G 13/7 NL

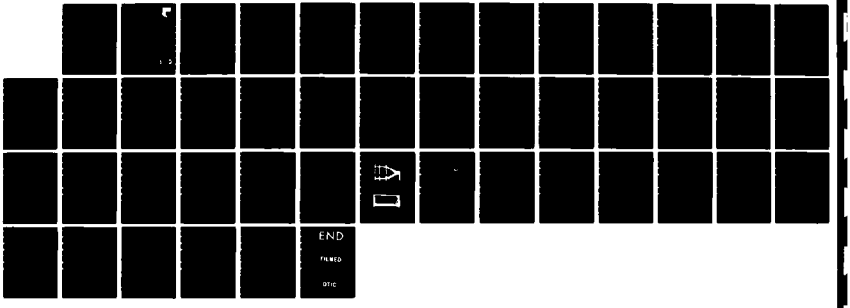

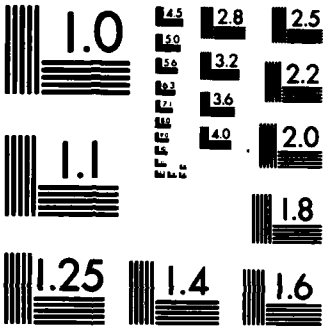

MICROCOPY RESOLUTION TEST CHART

AFWAL-TR-85-2039

DEVELOPMENT OF A NAVIER-STOKES ANALYSIS FOR THE FLOW IN DISK PUMPS

Y.-N. KIM
R. C. BUGGELN
H. MCDONALD

SCIENTIFIC RESEARCH ASSOCIATES, INC.
P. O. BOX 498
GLASTONBURY, CONNECTICUT 06033

APRIL 1985

FINAL REPORT FOR PERIOD SEPTEMBER 1984 - MARCH 1985

AERO PROPULSION LABORATORY
AIR FORCE WRIGHT AERONAUTICAL LABORATORIES
AIR FORCE SYSTEMS COMMAND
WRIGHT-PATTERSON AIR FORCE BASE, OHIO 45433

NOTICE

When Government drawings, specifications, or other data are used for any purpose other than in connection with a definitely related Government procurement operation, the United States Government thereby incurs no responsibility nor any obligation whatsoever; and the fact that the government may have formulated, furnished, or in any way supplied the said drawings, specifications, or other data, is not to be regarded by implication or otherwise as in any manner licensing the holder or any other person or corporation, or conveying any rights or permission to manufacture use, or sell any patented invention that may in any way be related thereto.

This report has been reviewed by the Office of Public Affairs (ASD/PA) and is releasable to the National Technical Information Service (NTIS). At NTIS, it will be available to the general public, including foreign nations.

This technical report has been reviewed and is approved for publication.

Richard J Martin

RICHARD J. MARTIN
Project Engineer

WALKER H. MITCHELL
Chief, Technology Branch
Turbine Engine Division
Aero Propulsion Laboratory

FOR THE COMMANDER

H I Bush

H. I. BUSH
Director
Turbine Engine Division
Aero Propulsion Laboratory

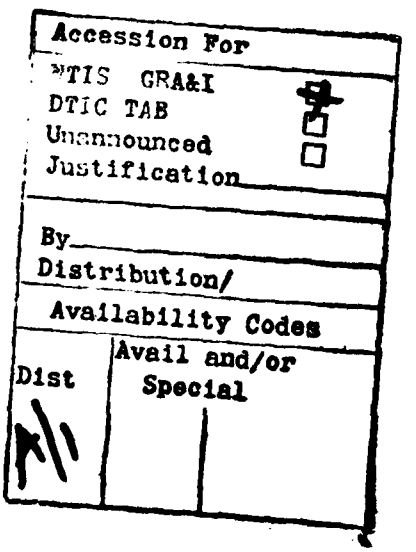

"If your address has changed, if you wish to be removed from our mailing list, or if the addressee is no longer employed by your organization please notify AFWAL/POTX, W-PAFB, OH 45433 to help us maintain a current mailing list".

Copies of this report should not be returned unless return is required by security considerations, contractual obligations, or notice on a specific document.

UNCLASSIFIED

SECURITY CLASSIFICATION OF THIS PAGE

REPORT DOCUMENTATION PAGE

1a. REPORT SECURITY CLASSIFICATION Unclassified	1b. RESTRICTIVE MARKINGS N/A
2a. SECURITY CLASSIFICATION AUTHORITY N/A	3. DISTRIBUTION/AVAILABILITY OF REPORT Approved for public release, distribution unlimited.
2b. DECLASSIFICATION/DOWNGRADING SCHEDULE N/A	
4. PERFORMING ORGANIZATION REPORT NUMBER(S) 910008F	5. MONITORING ORGANIZATION REPORT NUMBER(S) AFWAL-TR-85-2039
6a. NAME OF PERFORMING ORGANIZATION Scientific Research Associates, Inc. 6b. OFFICE SYMBOL (If applicable)	7a. NAME OF MONITORING ORGANIZATION Aero Propulsion Laboratory (AFWAL/POTX) Air Force Wright Aeronautical Laboratories
6c. ADDRESS (City, State and ZIP Code) P.O. Box 498 Glastonbury, CT 06033	7b. ADDRESS (City, State and ZIP Code) Wright Patterson AFB, OH 45433
8a. NAME OF FUNDING/SPONSORING ORGANIZATION Aero Propulsion Laboratory Air Force Wright Aeronautical 8b. OFFICE SYMBOL (If applicable) AFWAL/XRPP	9. PROCUREMENT INSTRUMENT IDENTIFICATION NUMBER F33615-84-C-2469
8c. ADDRESS (City, State and ZIP Code) Wright Patterson Air Force Base, OH 45433	10. SOURCE OF FUNDING NOS. PROGRAM ELEMENT NO.: 65502F; PROJECT NO.: 3004; TASK NO.: 20; WORK UNIT NO.: 19
11. TITLE (Include Security Classification) Development of a Navier-Stokes Analysis for the Flow in Disk Pumps	
12. PERSONAL AUTHOR(S) Y.-N. Kim, R.C. Buggeln and H. McDonald	
13a. TYPE OF REPORT Final 13b. TIME COVERED FROM 9/84 TO 3/85	14. DATE OF REPORT (Yr., Mo., Day) April 1985 15. PAGE COUNT 45
16. SUPPLEMENTARY NOTATION	
17. COSATI CODES FIELD / GROUP / SUB. GR.	18. SUBJECT TERMS (Continue on reverse if necessary and identify by block number) Disk Pumps, Navier-Stokes Equations, Computational Fluid Mechanics, Alternating Direction Implicit.

19. ABSTRACT (Continue on reverse if necessary and identify by block number)

A technique has been developed to solve the Navier-Stokes equations for the flow in disk pumps. The technique uses a linearized block implicit-alternating direction technique to efficiently solve the unsteady governing equations to a steady state with appropriate boundary conditions and initial conditions. The resulting code was used to calculate the flow in two different geometries under the same flow conditions. Demonstration calculation indicates that the code will be a valuable tool in analytically evaluating the performance of existing and future disk pumps.

20. DISTRIBUTION/AVAILABILITY OF ABSTRACT UNCLASSIFIED/UNLIMITED ☐ SAME AS RPT. ☒ DTIC USERS ☐	21. ABSTRACT SECURITY CLASSIFICATION Unclassified
22a. NAME OF RESPONSIBLE INDIVIDUAL Richard J. Martin	22b. TELEPHONE NUMBER (Include Area Code) (513) 255-6720 22c. OFFICE SYMBOL AFWAL/XRPP

DD FORM 1473, 83 APR EDITION OF 1 JAN 73 IS OBSOLETE.

Unclassified

SECURITY CLASSIFICATION OF THIS PAGE

TABLE OF CONTENTS

INTRODUCTION

In the high temperature environment of advanced high performance turbines of interest to the Air Force, cooling air and its associated cost becomes a critical item. Typically cooling air is bled from the compressor and delivered to the turbine through the machine core out of the primary gas path and circumventing the combustor. Provided the cooling air is discharged into the turbine sufficiently early, the major losses are incurred in the off gas path flow and delivery system. These losses can be an appreciable cost in overall efficiency when the cooling mass flow requirements become a significant fraction of the primary gas flow, as occurs in most high temperature high performance engines. Taking the bleed flow out of the gas path and delivering it to the turbine with little loss in total pressure turns out to be a difficult task. Furthermore, the cooling air can be required also to cool the turbine disks prior to or in addition to, cooling the turbine rotor or vane blades.

A major problem that can arise in this cooling air delivery process is associated with ability of the rotor disk to pump the cooling air out into the gas path. The so-called 'disk pumping problem' arises in part by virtue of the shear stress on the rotating disk. This is in itself a drag producing mechanism. Enough air is required to be driven out in the gas path to prevent ingestion of the hot main gas flow into the disk cavity. However, the amount involved should not be so much as to adversely thicken the endwall boundary layers or to otherwise disrupt the primary gas flow. Furthermore, it is desirable on an overall basis to minimize the coolant mass flow requirements.

Further complications can arise by virtue of modern turbine design which take advantage of the structural savings which result from hanging the stators from the casing, as is shown schematically in Fig. 1. The axial static pressure drop in the turbine requires the stator to be sealed and one possible method is shown in Fig. 1. Under certain conditions the resulting configuration may allow ingestion of the hot main flow gas into the cavity such as in cavity "d", and special care is required to inhibit or prevent this process. Clearly the problems of disk pumping, disc cooling and overall interaction with the main gas path are complex. In view of their importance to structural integrity, durability and efficiency it would be very desirable to have a good understanding and predictive capability for these flows.

Insofar as the analysis is concerned, unfortunately the complex turbulent recirculating rotational nature of the flow does not permit significant simplification in developing a mathematical approach, and consequently to date very little has been done in the way of developing formal analyses for this problem from the basic governing equations. Various geometry dependent variations of the disk pump concept can arise, however, only a limited amount of experimental data for these various possible configurations is available. Hence, an analysis capable of accurately and efficiently predicting disk cavity flows would be a major tool for both the research and design engineers. The initial development of such a program was the major focus of the present Phase I effort.

Considering that the disk pump may operate under the possible recirculating and turbulent flow conditions, it is clear that the solution of the ensemble-averaged Navier-Stokes equations represent the appropriate approach to the problem. However, accurate and efficient solutions of the Navier-Stokes equations in complex geometries for realistic flow conditions represent a formidable task. Recently, Buggeln and McDonald (Ref. 1) have successfully solved the Navier-Stokes equations for a variety of labyrinth seal configurations at realistic flow conditions, and have obtained results which show good agreement with experimental measurements. Although the disk pumping problem differs from the labyrinth seal problem, it was felt that this same procedure with modification could be used as an accurate and efficient approach to the disk pumping problem. Therefore, under the present Phase I effort, the work focused upon demonstrating and assessing the applicability of a modified version of this labyrinth seal computer code to the problem of the flow in a disk pumping cavity of type d in Fig. 1.

In the present study an axisymmetric configuration was supposed for the disk pump, and this is considered a good approximation for the present program since the axisymmetric configuration gives rise to the relevant physical flow phenomena. It should be noted that the axisymmetric configuration permits swirling cavity flows to arise, but would not treat a discretely three-dimensional proturberance, such as a bolt head. Fully three-dimensional flows, although possible to compute with this type of analysis (e.g. Refs. 2 and 3), would require considerably more computer run time than axisymmetric flows. Therefore, since the present effort was to concentrate upon assessing the potential of the approach, it was decided not

to pursue three-dimensional flows under Phase I of the effort. Three-dimensional flows as well as other complicating factors could be performed on a Phase II effort.

In order to demonstrate the ability to analyze simple disk pumping flows, the present effort concentrated on predicting the flow in a cavity of the type d shown in Fig. 1. In this type of cavity one disk wall is fixed, the other rotating. Air enters along the disk inner radius wall and leaves along the disk periphery. The final model disk/cavity configurations actually utilized in the present study are shown in Fig. 2. Although somewhat simplified, it represents a viable approximation to actual geometries.

This report presents and describes the analysis of disk pumping flows based on the linearized block implicit (LBI) technique for the numerical solution of the multidimensional, time-dependent Navier-Stokes equations by Briley and McDonald (Ref. 4). Two different shapes of disk pump were considered in the demonstration calculation (Fig. 2). In the following sections, a general description of the present analysis, procedures, results and an assessment of the potential of the method are given.

ANALYSIS

Governing Equations

The equations used in the present effort are the ensemble-averaged, time-dependent Navier-Stokes equations which can be written in vector form as

Continuity

$$\frac{\partial \rho}{\partial t} + \nabla \cdot \rho \vec{u} = 0 \tag{1}$$

Momentum

$$\frac{\partial \rho \vec{u}}{\partial t} + \nabla \cdot (\rho \vec{u}\vec{u}) = - \nabla p + \nabla \cdot (\bar{\bar{\pi}} + \pi^T) \tag{2}$$

Energy

$$\frac{\partial \rho h}{\partial t} + \nabla \cdot (\rho \vec{u} h) = - \nabla \cdot (\vec{q} + \vec{q}^T) + \frac{Dp}{Dt} + \Phi + \rho \varepsilon \tag{3}$$

where ρ is density, $\vec{u}$ is velocity, p is pressure, $\bar{\bar{\pi}}$ is the molecular stress tensor, π^T is the turbulent stress tensor, h is enthalpy, $\vec{q}$ is the mean heat flux vector, $\vec{q}^T$ is the turbulent heat flux vector, Φ is the mean flow dissipation rate and ε is the turbulence energy dissipation rate. If the flow is assumed to have a constant total temperature, the energy equation is replaced by

$$T_o = T + \frac{q^2}{2C_p} = \text{constant} \tag{4}$$

where T_o is the stagnation temperature, q is the magnitude of the velocity and C_p is the specific heat at constant pressure. In both cases considered in this work the assumption of constant total temperature has been invoked by using Eq. 4 as an approximation to Eq. 3 for the sole purpose of reducing computer run time where the constant T_o assumption was warranted.
A number of terms appearing in Eqs. 1-4 require definition. The stress tensor appearing in Eq. 2 is defined as

$$\bar{\bar{\pi}} = 2\mu \mathbb{D} - \left(\frac{2}{3}\mu - K_B\right) \nabla \cdot \vec{U}\, \mathbb{I} \tag{5}$$

where K_B is the bulk viscosity coefficient and $\mathbb{D}$ is the deformation tensor, defined by:

$$\mathbb{D} \equiv \frac{1}{2}\left((\nabla\vec{U}) + (\nabla\vec{U})^T\right) \tag{6}$$

In addition the turbulent stress tensor has been modeled using an isotropic eddy viscosity such that:

$$\pi^T = -\rho\, \overline{\vec{u}'\,\vec{u}'} = 2\mu_T \tag{7}$$

where μ_T, the turbulent viscosity, is determined by a suitable turbulence model. Turbulence modeling is described in some detail later.

Equation 3 contains a mean heat flux vector defined as follows:

$$\vec{q} = -\kappa\,(\nabla T) \tag{8}$$

and a turbulent heat flux vector defined as:

$$\vec{q}^T = -\kappa^T\,(\nabla T) \tag{9}$$

where κ and κ^T are the molecular (laminar) and turbulent thermal conductivities, respectively.

Also appearing in Eq. 3 is the mean flow dissipation term Φ.

$$\Phi = 2\mu \, \mathbb{D} : \mathbb{D} - \left(\frac{2}{3}\mu - K_B\right)(\nabla \cdot \vec{U})^2 \tag{10}$$

The equation of state for a perfect gas

$$p = \rho RT \tag{11}$$

where R is the gas constant, the caloric equation of state

$$e = c_v T \tag{12}$$

and the definition of static enthalpy

$$h = c_p T \tag{13}$$

supplement the equations of motion.

Finally the flow properties μ, κ and K_B are determined using the following constitutive relations.

The molecular viscosity μ is determined using Sutherland's law.

$$\frac{\mu}{\mu_o} = \left(\frac{T}{T_o}\right)^{3/2} \frac{T_o + S_1}{T + S_1} \tag{14}$$

where $S_1 = 100°K$ for air.

The bulk viscosity will be assumed to be zero,

$$K_B = 0 \tag{15}$$

and the thermal conductivity may be determined by use of a relation similar to Sutherland's law viz.

$$\frac{\kappa}{\kappa_o} = \left(\frac{T}{T_o}\right)^{3/2} \frac{T_o + S_2}{T + S_2} \tag{16}$$

where $S_2 = 194°K$ for air.

Turbulence Modeling

Three possible turbulence models are contained within the disk pump code. These are (i) zero equation model - (mixing length model), (ii) one-equation model - (a turbulence energy-algebraic length scale model), and (iii) two-equation model - (a turbulence energy-turbulence dissipation model). Among these models (i) and (iii) were included in the computation. Therefore, a detailed explanation would be given to only (i) and (iii).

Zero Equation Model - (Mixing Length)

Of all available turbulence models, Prandtl's mixing length model is probably still the most widely used. The model was originally developed for use in unseparated boundary layer flow situations and has been shown to perform well under such conditions. In the cases described in this report the mixing length model has ben used during the early transient period of flow development in a disk pump. An advantage of the method from the point of view of economy is that is does not require additional transport equations to model the effect of turbulence, but rather relates the Reynold's shear stress to mean flow quantities via:

$$\overline{\rho u_i' u_j'} = \frac{\mu_T}{R_e} \frac{\partial U_j}{\partial x_i} \tag{17}$$

where

$$\frac{\mu_T}{Re} = \rho \ell^2 (2 \, \mathbb{D} : \mathbb{D})^{1/2}$$

where

$$\ell = \min[\ell_\infty, \kappa d D]$$

where d is the normal distance to the nearest wall and D is van Driest damping coefficient given by

$$\begin{aligned} D &= 1 - \exp(- y^+/A^+) \\ \ell_\infty &= 0.09\delta \\ \kappa &= 0.4 \\ y^+ &= d u_\tau/\nu \end{aligned} \tag{18}$$

$$u_\tau = (\tau_\ell/\rho)^{1/2} \tag{19}$$

where the local shear stress τ_ℓ is obtained from

$$\tau_\ell = (2\ \mathbb{D} : \mathbb{D}\ )^{1/2}$$

and $\mathbb{D}$ is defined by Eq. 6.

One problem in the mixing length formulation is the definition of δ. In boundary layers the streamwise velocity u approaches an edge velocity, u_e, asymptotically. However, a monotonic approach to an asymptotic edge velocity is not characteristic of Navier-Stokes solutions particularly in complicated recirculating flows such as that would be considered in the present report. In order to avoid the problem of determining the boundary layer edge, δ, as defined in the usual boundary layer context, i.e., δ is the distance from the wall at which $u/u_e = 0.99$, the following relation is used.

$$\delta = 2.0 d_{(q/q_{max}=c)} \tag{20}$$

In other words, δ, is taken as twice the distance (measured away from the nearest wall) for which $q/q_{max} = c$. The value of c used in the present effort was 0.90.

Two-Equation Model - (k-ε)

The k-ε, two-equation turbulence model [6, 7] in which both the turbulence kinetic energy and the turbulence dissipation rate are governed by transport equations represents a more general model. In this approach the k-equation is as given by:

$$\frac{\partial(\rho k)}{\partial t} + \nabla \cdot (\rho \vec{U} k) = \nabla \cdot \frac{\mu_T}{\sigma_k} \nabla k + 2\mu_T\ (\ \mathbb{D} : \mathbb{D}\ ) - \rho\varepsilon - 2\rho\nu \left(\nabla k^{1/2}\right)^2 \tag{21}$$

and the ε-equation by:

$$\frac{\partial(\rho\varepsilon)}{\partial t} + \nabla\cdot(\rho\vec{u}\varepsilon) = \nabla\cdot\left(\frac{\mu_T}{\sigma_\varepsilon}\ \nabla\varepsilon\right) + c_1(2\mu_T\ \mathbb{D}:\mathbb{D}\ ) + 2\mu\mu_T(\nabla^2 U)^2 - c_2\rho\ \frac{\varepsilon}{k} \tag{22}$$

where following Reference 6

$$c_1 = 1.55$$

and

$$c_2 = c_{2\infty}\ \ [1 - 0.3\ \exp(-R_T)^2] \tag{23}$$

$$c_{2\infty} = 2.0$$

and R_T is defined as:

$$R_T = \frac{\rho k^2}{\varepsilon \mu} \tag{24}$$

However, attempts to solve Eqs. 21 and 22 without modification fail because an appropriate boundary condition for ε at a solid boundary is difficult to prescribe such that Eq. 22 is satisfied. In order to circumvent this problem, Eq. 22, the turbulence dissipation equation, has been modified by the inclusion of the term:

$$- 2\mu\mu_T \left(\nabla^2 U\right)^2 \tag{25}$$

As discussed by Jones and Launder (Ref. 6) inclusion of this term leads to better agreement with experimentally measured k distributions in the near-wall region. In addition, Jones and Launder's (Ref. 6) inclusion of the term:

$$- 2\rho\nu \left(\nabla k^{1/2}\right)^2 \tag{26}$$

in Eq. 21 is a device which models new wall dissipation and thus allows ε=0 to be prescribed as a function boundary condition.

Transformation of Governing Equations

The governing equations for the present problems have been given in the previous section in vector form (Eqs. 1 - 3 and 21 - 22). However, implementation of a solution procedure requires that these equations be transformed into an appropriate coordinate system. Therefore, the governing equations written in a cylindrical-polar coordinate system are transformed with a general Jacobian transformation of the form

$$\begin{aligned} y^j &= y^j(\bar{x}_1, \bar{x}_2, \bar{x}_3, t) \\ \tau &= t \end{aligned} \tag{27}$$

where $(\bar{x}_1, \bar{x}_2, \bar{x}_3) = (r, \Theta, z)$ are the original cylindrical polar coordinates. The velocity components remain the components (U_1, U_2, U_3) in the $(\bar{x}_1, \bar{x}_2, \bar{x}_3)$ coordinate directions, respectively. The new independent variables y^j are the computational coordinates in the transformed system.

Application of the Jacobian transformation requires expansion of the temporal and spatial derivatives using the chain rule, i.e.,

$$\frac{\partial \phi}{\partial t} = \frac{\partial \phi}{\partial \tau} + \sum_{j=1}^{3} y^j_{,t} \frac{\partial \phi}{\partial y^j} \tag{28}$$

and

$$\frac{\partial \phi}{\partial \bar{x}_i} = \sum_{j=1}^{3} y^j_{,i} \frac{\partial \phi}{\partial y^j} \tag{29}$$

where

$$y^j_{,t} \equiv \frac{\partial y^j}{\partial t}$$

$$y^j_{,i} \equiv \frac{\partial y^j}{\partial \bar{x}_i} \tag{30}$$

The relations Eqs. 29 - 30 are first substituted into the governing equations written in cylindrical polar coordinates. Then the resulting equations are multiplied by the Jacobian determinant of the inverse transformation,

$$J = \frac{\partial(\bar{x}_1, \bar{x}_2, \bar{x}_3)}{\partial(y^1, y^2, y^3)} = \begin{vmatrix} \frac{\partial \bar{x}_1}{\partial y^1} & \frac{\partial \bar{x}_1}{\partial y^2} & \frac{\partial \bar{x}_1}{\partial y^3} \\ \frac{\partial \bar{x}_2}{\partial y^1} & \frac{\partial \bar{x}_2}{\partial y^2} & \frac{\partial \bar{x}_2}{\partial y^3} \\ \frac{\partial \bar{x}_3}{\partial y^1} & \frac{\partial \bar{x}_3}{\partial y^2} & \frac{\partial \bar{x}_3}{\partial y^3} \end{vmatrix} \tag{31}$$

and the equations are cast into a conservative form using the following relations

$$\sum_{j=1}^{3} \frac{\partial \hat{y}^j_{,i}}{\partial y^j} = 0 \tag{32}$$

$$\frac{\partial J}{\partial \tau} + \sum_{j=1}^{3} \frac{\partial \hat{y}^j}{\partial y^j}_{,t} = 0 \tag{33}$$

where

$$\hat{y}^j{}_{,i} \equiv J y^j{}_{,i}$$
$$\hat{y}^j{}_{,t} \equiv J y^j{}_{,t} \tag{34}$$

It should be noted that Equation 33 expresses a geometric conservation law and plays an important role in enabling the equations of motion to be cast into conservative form.

The particular conservation form developed implies that all factors involving the radial coordinate $r = \bar{x}_1$ remain as they were before the Jacobian transformation. The resulting equations are presented below as Eqs. 37 - 46.

The geometric relations Eq. 32 - 33 may be obtained from the transformation relations for $\hat{y}^j_{,t}$ and $\hat{y}^j_{,i}$ in terms of the inverse transformation derivatives

$$\hat{y}^1{}_{,1} = \bar{x}_{2,2}\,\bar{x}_{3,3} - \bar{x}_{2,3}\bar{x}_{3,2}$$
$$\hat{y}^1{}_{,2} = \bar{x}_{3,2}\,\bar{x}_{1,3} - \bar{x}_{3,3}\,\bar{x}_{1,2}$$
$$\hat{y}^1{}_{,3} = \bar{x}_{1,2}\,\bar{x}_{2,3} - \bar{x}_{1,3}\,\bar{x}_{2,2}$$
$$\hat{y}^2{}_{,1} = \bar{x}_{2,3}\,\bar{x}_{3,1} - \bar{x}_{2,1}\,\bar{x}_{3,3}$$
$$\hat{y}^2{}_{,2} = \bar{x}_{3,3}\,\bar{x}_{1,1} - \bar{x}_{3,1}\,\bar{x}_{1,3} \tag{35}$$
$$\hat{y}^2{}_{,3} = \bar{x}_{1,3}\,\bar{x}_{2,1} - \bar{x}_{1,1}\,\bar{x}_{2,3}$$
$$\hat{y}^3{}_{,1} = \bar{x}_{2,1}\,\bar{x}_{3,2} - \bar{x}_{2,2}\,\bar{x}_{3,1}$$
$$\hat{y}^3{}_{,2} = \bar{x}_{3,1}\,\bar{x}_{1,2} - \bar{x}_{3,2}\,\bar{x}_{1,1}$$
$$\hat{y}^3{}_{,3} = \bar{x}_{1,1}\,\bar{x}_{2,2} - \bar{x}_{1,2}\,\bar{x}_{2,1}$$

$$\hat{y}^j{}_{,t} = -\sum_{k=1}^{3} \hat{y}^j{}_{,k} \frac{\partial \bar{x}_k}{\partial \tau} \tag{36}$$

The transformed governing equations may be written in the following compact form:

$$\frac{\partial(J\vec{W})}{\partial \tau} = -\sum_{j=1}^{3} \frac{\partial}{\partial y^j} (Jy^j{}_{,t}\vec{W}) - \sum_{j=1}^{3} \left(\beta_i \frac{\partial}{\partial y^j} (Jy^j{}_{,i}\vec{F}_i)\right.$$

$$\left. + \gamma_i \frac{\partial}{\partial y^j} (Jy^j{}_{,i}\vec{P}_i) + \zeta_i \frac{\partial}{\partial y^j} (Jy^j{}_{,i}\vec{G}_i)\right) \tag{37}$$

$$+ J\vec{S} + J\vec{C}$$

where

$$y,^j_t \equiv \frac{\partial y^j}{\partial t}$$

$$y,^j_i \equiv \frac{\partial y^j}{\partial \bar{x}_i} \tag{38}$$

Further, the coefficients β_i, γ_i, ζ_i are given by

$$\beta_1 = \frac{1}{r}, \quad \beta_2 = \frac{1}{r}, \quad \beta_3 = 1$$

$$\gamma_1 = 1, \quad \gamma_2 = \frac{1}{r}, \quad \gamma_3 = 1 \tag{39}$$

$$\zeta_1 = \frac{1}{r^m}, \quad \zeta_2 = \frac{1}{r}, \quad \zeta_3 = 1$$

and m = 1 for all equations except the x_2 - direction momentum equation,

for which m = 2. The vector variables used in Eq. 37 are defined as

$$\vec{W} = \begin{bmatrix} \rho U_1 \\ \rho U_2 \\ \rho U_3 \\ \rho \\ \rho h \\ \rho k \\ \rho \varepsilon \end{bmatrix} \qquad \vec{F}_i = r^n \begin{bmatrix} \rho U_1 U_i \\ \rho U_2 U_i \\ \rho U_3 U_i \\ \rho U_i \\ \rho h U_i \\ \rho k U_i \\ \rho \varepsilon U_i \end{bmatrix} \tag{40}$$

where n = 1 for i = 1 and n = 0 for i = 2, 3.

$$\vec{P}_i = \begin{bmatrix} p\delta_{i1} \\ p\delta_{i2} \\ p\delta_{i3} \\ 0 \\ 0 \\ 0 \\ 0 \end{bmatrix} \qquad \vec{G}_1 = \begin{bmatrix} r\tau_{11} \\ r^2\tau_{12} \\ r\tau_{13} \\ 0 \\ -rq_1 \\ \frac{\mu_T}{\sigma_k} \gamma_1 k_{,1} \\ \frac{\mu_T}{\sigma_\varepsilon} \gamma_1 \varepsilon_{,1} \end{bmatrix} \tag{41}$$

$$G_i = \begin{bmatrix} \tau_{i1} \\ \tau_{i2} \\ \tau_{i3} \\ 0 \\ q_i \\ \frac{\mu_T}{\sigma_k} \gamma_i k_{,i} \\ \frac{\mu_T}{\sigma_\varepsilon} \gamma_i \varepsilon_{,i} \end{bmatrix} \qquad \text{for } i = 2,3$$

Note that the velocity components (U_1, U_2, U_3) are the cylindrical-polar velocity components, and τ_{ij} is the stress tensor written in cylindrical-polar coordinates. The molecular and turbulent stress tensors may be written as

$$\tau_{ij} = 2\mu_{eff}\,\bar{D}_{ij} \tag{42}$$

$$\bar{D}_{11} = \frac{\partial U_1}{\partial \bar{x}_1}$$

$$\bar{D}_{22} = \frac{1}{r}\frac{\partial U_2}{\partial \bar{x}_2} + \frac{U_1}{r}$$

$$\bar{D}_{33} = \frac{\partial U_3}{\partial \bar{x}_3} \tag{43}$$

$$\bar{D}_{12} = \frac{1}{2}\left[r\frac{\partial}{\partial \bar{x}_1}\left(\frac{U_2}{r}\right) + \frac{1}{r}\frac{\partial U_1}{\partial \bar{x}_2} \right]$$

$$\bar{D}_{13} = \frac{1}{2}\left[\frac{\partial U_3}{\partial \bar{x}_1} + \frac{\partial U_1}{\partial \bar{x}_3} \right]$$

$$\bar{D}_{23} = \frac{1}{2}\left[\frac{1}{r}\frac{\partial U_3}{\partial \bar{x}_2} + \frac{\partial U_2}{\partial \bar{x}_3} \right]$$

$$\nabla \cdot \bar{U} = \frac{1}{r}\frac{\partial}{\partial \bar{x}_1}(rU_1) + \frac{1}{r}\frac{\partial U_2}{\partial \bar{x}_2} + \frac{\partial U_3}{\partial \bar{x}_3} \tag{44}$$

The derivatives required in Eqs. 43 - 44 must be expressed in terms of the computational coordinates y^j using the chain rule, (Eq. 29).

Finally, the vector $\vec{S}$ contains source terms and certain differential terms which do not conform to the basic structure of Eq. 37, and the vector $\vec{C}$ contains the additional curvature terms due to the cylindrical-polar coordinate system.

$$\vec{S} = \begin{bmatrix} 0 \\ 0 \\ 0 \\ 0 \\ \frac{Dp}{Dt} + \Phi + \rho\varepsilon \\ \mu_T \left[2\bar{D}_{ij}\,\bar{D}_{ij}\right] - \rho\varepsilon - 2\rho\nu\,(\nabla k^{1/2})^2 \\ C_1 \frac{\varepsilon}{k}\left[\mu_T(2\bar{D}_{ij}\,\bar{D}_{ij}) + 2\,\mu\mu_T\,(\nabla^2 U)^2 - C_2\,\rho\,\frac{\varepsilon^2}{k}\right] \end{bmatrix} \tag{45}$$

$$\vec{C} = \begin{bmatrix} \frac{1}{r}\rho U_2^{\,2} - \frac{1}{r}\,\bar{\tau}_{22} \\ -\frac{1}{r}\rho U_1 U_2 \\ 0 \\ 0 \\ 0 \\ 0 \\ 0 \end{bmatrix} \tag{46}$$

Numerical Procedure

The numerical procedure used to solve the governing equations is a consistently split linearized block implicit (LBI) scheme originally developed by Briley and McDonald (Ref. 4). A conceptually similar scheme has been developed for two-dimensional MHD problems by Lindemuth and Killeen (Ref. 9). The procedure is discussed in detail in Refs. 4 and 5. The method can be briefly outlined as follows: the governing equations are replaced by

an implicit time difference approximation, optionally a backward difference or Crank-Nicolson scheme. Terms involving nonlinearities at the implicit time level are linearized by Taylor series expansion in time about the solution at the known time level, and spatial difference approximations are introduced. The result is a system of multidimensional coupled (but linear) difference equations for the dependent variables at the unknown or implicit time level. To solve these difference equations, the Douglas-Gunn (Ref. 10) procedure for generating alternating-direction implicit (ADI) schemes as perturbations of fundamental implicit difference schemes is introduced in its natural extension to systems of partial differential equations.
This technique leads to systems of coupled linear difference equations having narrow block-banded matrix structures which can be solved efficiently by standard block-elimination methods.

The method centers around the use of a formal linearization technique adapted for the integration of initial-value problems. The linearization technique, which requires an implicit solution procedure, permits the solution of coupled nonlinear equations in one space dimension (to the requisite degree of accuracy) by a one-step noniterative scheme. Since no iteration is required to compute the solution for a single time step, and since only moderate effort is required for solution of the implicit difference equations, the method is computationally efficient; this efficiency is retained for multidimensional problems by using what might be termed block ADI techniques. The method is also economical in terms of computer storage, in its present form requiring only two time-levels of storage for each dependent variable. Furthermore, the block ADI technique reduces multidimensional problems to sequences of calculations which are one-dimensional in the sense that easily-solved narrow block-banded matrices associated with one-dimensional rows of grid points are produced. A more detailed discussion of the solution procedure as discussed by Briley, Buggeln and McDonald (Ref. 11) is given in the Appendix A.

CURRENT EFFORTS

Objective

A primary objective of the current efforts was to demonstrate the ability of a modified version of the labyrinth seal code to be applied to a disk pumping cavity of the type d in Fig. 1. Since the present Phase I work focused upon demonstration and assessment, model axisymmetric cavity shapes were considered. This configuration allows swirling flows in the cavity although the computation is performed in two dimensions since no azimuthal variation is assumed. The current type of disk pump operates with one cavity wall fixed, while the other rotating. Air enters at a location near the inner radius, and leaves along the disk periphery as shown in Fig. 2. The disk periphery was assumed to be an exit boundary in the sense that air was not permitted to enter the cavity from the free stream and similarly flow within the cavity was not permitted to leave via the inlet on the axis of rotation. As shall be discussed, the specific objectives under the Phase I effort have been met completely.

Coordinate System

The coordinate system is an important component of the Navier-Stokes analysis. An inappropriate coordinate system may lead to difficulty in obtaining a converged solution and even exhibit physically unrealistic predictions due to geometric truncation error. Therefore, generation f a viable system is mandatory. Any coordinate system used in the analysis should satisfy conditions of (i) generality, (ii) smoothness, (iii) resolvability and (iv) allow easy application of boundary conditions. Obviously, a coordinate system must be sufficiently general to allow application to a wide class of problems of interest if it is to be practical. The metric data associated with the coordinte system must be sufficiently smooth so that the variation from grid point to grid point does not lead to a numerical solution dominated by metric coefficient truncation error; it should be noted that this requirement differs from the requirement of the existence of a specified number of transformation derivatives. The coordinate system must resolve flow regions where rapid flow field change occurs. Finally, coordinates should allow accurate implementation of

boundary conditions. The specification of boundary surfaces which do not fall upon coordinate lines or at specific grid points may present a difficult problem for Navier-Stokes analyses. The problem is considerably more severe in viscous flows where no-slip conditions on solid walls can combine with boundary condition truncation error to produce numerical solutions which are both qualitatively and quantitatively in error. Thus, the property required of any coordinate system to be used in a viscous analysis should be that boundary surfaces fall on coordinate lines. Such a system is called a body-fitted coordinate system.

Many alternative approaches are available for generating body-fitted coordinates, although in general they can be categorized into three generic groups. These are conformal, algebraic and elliptic. Conformal systems are based upon well known conformal transformation techniques. Algebraic or constructive techniques are typified by the method of Eiseman (Ref. 12) while methods using elliptic partial differential equations are in the main based on the work of Thompson, Thames and Mastin (Ref. 13). While the main advantage of the use of elliptic generation is that the method is applicable to complex geometries without the need to modify the basic approach for each new configuration, algebraic methods have the apparent advantage of conceptual simplicity for complex boundary geometries. In the present work the constructive approach has been adopted, although the Thompson approach is presently available at SRA and could be utilized in the future efforts associated with disk pump flow analysis.

In the case of plain disk cavity, the coordinate system is straightforward. A simple cylindrical coordiante system is utilized because of its axisymmetric shape as shown in Fig. 3. Horizontal lines represent the axial coordinate lines, while the radial coordinate lines are represented by transverse lines. Partly embedded solid regions were assumed within the domain of interest for coordinate generation. As a result, reentrant corners were generated. A further distribution of grid points within the computational domain is required to obtain high grid resolution in regions where rapid flow variations are expected. This is accomplished by use an analytical transformation technique developed by Oh (Ref. 14). The transformation function is composed of a series of complementary error functions. One of the advantages in the use of this transformation function lies in the capability of controlling the local grid points distribution

without effecting the distribution at other locations of interest. For further details of the technique, the reader should refer to Ref. 14.

On the other hand, the shaped disk cavity grid coordinate system requires a calculation or specification of arc lengths on the boundaries. Then, the distribution of grid points on and within the boundaries are obtained based on the parametrized arc length. The same transformation technique (Ref. 14) was used to pack the grid points in the region of large gradients in flow variables. The final coordinate systems used in the present work are shown in Fig. 3.

Navier-Stokes Analysis

Having generated a viable coordinate system, the next step in the process is to obtain a solution of the Navier-Stokes equations for the specified coordinate system and flow conditions. The analysis was performed in the same axisymmetric configurations as shown in Fig. 2. One of the cavity walls was assumed to rotate about the axis at 3600 rpm, while the other wall was stationary. The major parameters representing the turbine disk test conditions are axial and tangential Reynolds numbers. The axial Reynolds number is defined as $Re_z = \dot{m}/\pi\mu r_o$ where $\dot{m}$ is the mass flow rate through the inlet, μ is the laminar viscosity and r_o is the maximum radius of rig, while the tangential Reynolds number is defined as $Re_t = \frac{\rho\Omega r_o^2}{\mu}$ there ρ is the density, Ω is the angular velocity of rotating disk wall. The axial and tangential Reynolds number selected in the present analysis was 2.2×10^4, and 4.0×10^6, respectively. The laminar viscosity, μ, in the present analysis was 1.905×10^{-5} (Newton-sec/m^2). Other flow conditions were derived from both Reynolds numbers and laminar viscosity. Reference Mach number was M = 0.135, while the static pressure was estimated as 2.3197×10^5 (Newton/m^2). The static temperature of the stream was 312.4°K. Meanwhile, the static pressure at the exit boundary was assumed to be atmospheric. Thus, the ratio of exit static pressure to the inlet pressure was 2. Reference length used in the computation was the maximum radius of the rig which was 0.2794m. The same flow conditions were used for both plain and shaped disk pump cavity. To analyze the flow in both cavities 101 mesh points were distributed in the radial direction. In the axial direction, 60

mesh points were used for the plain cavity case, and 71 mesh points were used for the shaped cavity case. The grid points were tightly packed in the vicinity of solid walls to achieve the maximum resolution in the boundary layers. For both cases the continuity, three momenta equations and the constant stagnation enthalpy condition were used as governing equations. However, because of the axisymmetric flow configuration, (no change of flow variables in the azimuthal direction), the computation required only two directions (axial and radial direction).

Boundary Conditions

A major factor in obtaining efficient solutions for the Navier-stokes equations is specification of appropriate boundary conditions. Specification of boundary conditions at wall is relatively straightforward, but proper specification at inflow and outflow boundaries presents a more difficult problem. The present effort follows the work of Briley and McDonald (Ref. 15) who suggest examining the characterisistics of the inviscid problem for guidance at inflow and outflow boundaries. Appropriate boundary conditions which were set in the present calculations are as follows:

(i) Inlet (subsonic inflow) boundary -
Function condition on u_1-velocity (radial velocity)
Two-layer model on u_3-velocity (axial velocity) and static enthalpy
Second derivative of static pressure set to zero.

(ii) Exit (subsonic outflow) boundary -
Second derivative of u_1, u_3 set to zero
Static pressure specified.

(iii) Wall boundary -
No-slip on u_1 and u_3
Normal (to the wall) momentum equation
Function condition on u (zero on stationary wall and nonzero on rotating wall).

The so-called two-layer model used at the inflow boundary is essentially a total pressure boundary condition applied to the core flow with a specified boundary layer profile shape for the wall region. Matching the static pressure at the edge, defined by the first computational point from the wall at which $|u_3|/|u_3|_{max}$ was greater than or equal to 0.99 on the previous time step, enables calcuation of $|u_3|$ at this point. This provides the required normalizing value for the pre-specified boundary layer profile shape. Overall, the method provides a mechanism for drawing mass into the system in order to satisfy the downstream pressure given an upstream core total pressure. This specification corresponds to the usual wind tunnel experiment where stagnation conditions are set in an upstream reservoir and static pressure is set at some downstream location. Specification of an inlet mass flux could be accomplished indirectly by varying the downstream static pressure.

Calculation

Effective running of the disk pumping cavity problem requires a case running protocol to obtain rapid convergence. The basic strategy for running the code consists of several steps. First, initial conditions within the both cavities assumed stagnant flow. Then, as the specified exit pressure at the outflow boundary is lowered, mass flow is drawn through the inlet. Swirl was assumed to be zero, and a mixing length turbulence model was used initially to develop the basic flow pattern within the cavities without the complexities of a swirl equation or a two-equation turbulence model. Then two different methods were implemented for the plain and shaped disks. In the case of the plain disk, rotation effects was introduced before the two-equation turbulence model replaced the mixing-length model. On the other hand, in the case of the shaped disk, the order was reversed, i.e. the two-equation turbulence model was introduced before rotation effects. Both run protocols were successful and neither appeared to have a definite advantage over the other. In both cases two-equation turbulence model equations were initially solved with invariant mean flows to develop approximate turbulence energy and dissipation fields prior to coupling these fields with the mean flow. Then, finally all equations including the turbulence equations were solved simultaneously until a converged solution was obtained.

Although the present Navier-Stokes analysis can be used both for time-dependent and steady-state flow situations, the focus of the present investigation is the steady state solution. In such a case, it is not necessary to accurately follow the transient motion and indeed it may be advantageous from a computational efficiency view point not to follow the transient motion accurately, if this accelerates convergence to the steady state. The present approach utilizes the matrix conditioning technique of Refs. 16 and 17 to accelerate convergence to a steady state. Using the techniques described in Refs. 16 and 17, the convergence took 250 time steps for both plain and shaped disk, respectively. The CRAY CPU time required for the convergence of both cases was less than 2100 secs.

Results

The calcuated velocity, Mach number and stream function contours of two test cases are presented in Fig. 4 through Fig. 10. Since experimental data is not available for direct comparison, discussion will primarily focus on qualitative description of the essential physical features predicted by the computation. Although both dependent variable contours and flow streamlines are presented, the clearest picture of the generated flow can be obtained from the flow streamlines.

In the case of a plain disk pump, a large recirculating fluid motion is generated within the cavity as shown in Figs. 8 and 9. The flow pattern in the absence of wall rotation is basically determined by the convection of the fluid due to the pressure difference between inlet and exit. In the present work, the static pressure at the exit is one-half of the pressure at the inlet. When the effects of disk wall rotation are considered, the flow pattern change is apparent including the radial displacment of the recirculation region within the cavity as seen in Fig. 9. However, considering that the basic flow structure still remains the same with and without rotation, it is likely that centrifugal pumping action is not dominant over the effects of convection because of a relatively large pressure drop in this case.

The flow pattern within the shaped disk cavity in the absence of wall rotation is different from the plain case. It is likely that this difference is strongly dependent on the geometry (Fig. 9-10). Under the same

nonrotating and pressure condition as the plain disk case, the flow within the shaped disk contains only a small recirculation region in the vicinity of reentrant corner near the inlet. When the effects of rotation are considered, the flow within the cavity changes substantially as shown in Fig. 10. The centrifugal pumping action causes a considerable change in the flow field for the shaped disk pump case. Since such a complex fluid motion can be associated with many physical mechanisms, it may be too premature to draw a definite conclusion before further detailed parametric studies are performed. However, it is likely that centrifugal pumping action sweeps the fluid away in the radial outward direction near the rotating cavity wall and induces a large recirculating fluid motion. Velocity and Mach number contours as shown in Figs. 4-7 present the further details of flow structures associated with both disk pump shapes for the cases which include rotation. Of particular interest is the contours of swirling velocity component (V). The figure indicates that the convection is closely related to the faster transfer of the swirling component of momentum in the axial direction for both shapes of disk.

A major application of the rotor disk is to pump the cooling air out into the hot gas path. However, since the disk wall (rotating) is exposed to hot temperature environment, the fluids within the cavity especially in the vicinity of the rotating disk may heat up due to the heat transfer through the disk wall. As a result, not only cooling efficiency loss but also structural damage may arise. Comparison of flow pattern in both shapes indicate that the shaped disk is more efficient in preventing such a hot temperature region developing adjacent to the disk wall. In this regard it should be noted that the closeness of the streamlines indicates the speed of the flow. The contours in Fig. 8 clearly show a large recirculation region along the right side wall for the plain disk. Fluid trapped in this region will heat up and lose its cooling effectiveness. Hence, the right hand wall in the plain disk would be expected to be a region of high wall temperature. In the case of the rotating shaped disk, the situation is much more favorable as shown in Fig. 8. Here cooling problems may occur on the upper wall, however, both the right and left side walls appear to be in contact with relatively rapidly moving cooling fluid. It should be noted that rotation makes a major difference in the flow and heat transfer patterns for the shaped cavity. In view of the strong dependence of flow field within the

cavity on the shape of the disk wall, various geometric shapes should be explored to find an optimum shape of the disk pump.

ESTIMATES OF TECHNICAL FEASIBILITY

Under the present effort, an existing Navier-Stokes solver developed for the analysis of labyrinth seal has been extended and applied to demonstrate its capability for the disk pumping problem. Coordinate systems were generated by the constructive approach, and used successfully for both plain and shaped disk pumps. However, a more general elliptic solver has been developed at SRA to generate the coordinate systems for the complex geometry of the advanced seal. This coordinate generation code would be available for the future analysis of disk pump problems under the more complex geometric configuration (Fig. 11).

The Navier-Stokes code was used to calculate the disk pump flow fields for two cases. In order to reduce run time vectorization of the code was initiated under the current effort. The partially vectorized code reduced run times by factor of 2 when continuity equation and two momentum equations were solved. Even with an additional momentum equation, the run time was saved by 25% on CRAY-1 computer. Based upon other efforts at SRA, it is expected that full vectorization would reduce run times by a further factor of 5 to 10. Although in the present work a constant stagnation enthalpy relation was assumed, the current code does include an energy equation (although not optimized) and has been successfully used in heat transfer calculations (Ref. 18). With a partially vectorized code, the work done under the present effort has allowed steady disk pump flow fields to be generated in less than 2100 secs of CRAY CPU time, i.e., approximately $1200 at a commercially available rate.

The present effort has concentrated on the analysis of flow fields within the modeled cavity shapes. Because of the general nature of the Navier-Stokes code more complex disk pump configurations can be considered in the future (Fig. 11). For these cases the elliptic coordinate system solver would be used to generate the more complex configurations. Results obtained for flow within both cavities are very encouraging in verifying the capability of the Navier-Stokes procedure for such a practically important problem. Although not pursued in the present effort, the code cold be used to predict the heat transfer through the disk pump wall by solving energy equation.

The calculations completed under the Phase I effort gave physically realistic flow patterns, and showed the effect of cavity shape and wall rotation upon the flow field. The run times used were encouraging, and with full vectorization it is expected that this code could be used as a major tool for the understanding and in the design of disk cavity configurations including wall heat transfer effects.

REFERENCES

1. Buggeln, R.C., McDonald, H.: Development of a Navier-Stokes Analysis for Labyrinth Seals - Volume I: Analysis and Results (AFWAL-TR-85-). In preparation.

2. Briley, W.R., Buggeln, R.C. and McDonald, H.: Solution of the Three-Dimensional Navier-Stokes Equations for a Steady Horseshoe Vortex Flow. SRA Report R84-920014-F, 1984.

3. Weinberg, B.C., Yang, R.-J., McDonald, H. and Shamroth, S.J.: Calculation of Two- and Three-Dimensional Transonic Cascade Flow Fields Using the Navier-Stokes Equations, ASME Paper 85-GT-66.

4. Briley, W.R. and McDonald, H.: Solution of the Multidimensional Compressible Navier-Stokes Equations by a Generalized Implicit Method, J. Comp. Physics, Vol. 24, No. 4, August 1977, p. 372.

5. Briley, W.R. and McDonald, H.: On the Structure and Use of Linearized Block Implicit Schemes, J. of Comp. Physics, Vol. 34, 1980, pp. 54-73.

6. Jones, W.P. and Launder, B.E.: The Prediction of Laminarization with a Two-Equation Model of Turbulence, Int. J. of Heat Mass Transfer, Vol. 15, 1972.

7. Patel, V.C., Rodi, W. and Scheurer, G.: Evaluation of Turbulence Models for Near-Wall and Low-Reynolds Number Flows, 3rd Symposium on Turbulent Shear Flows, Universtiy of California, Davis, September 1983.

8. Thomas, P.D. and Lombard, C.K.: Geometric Conservation Law and its Application to Flow Computations on Moving Grids, AIAA Journal, Vol. 17, No. 10, pp. 1030-1037, 1979.

9. Lindemuth, I. and Killeen, J.: Alternating Direction Implicit Techniques for Two-Dimensional Magnetohydrodynamic Calculations, J. of Comp. Physics, Vol. 13, 1973.

10. Douglas, J. and Gunn, J.E.: A General Formulation of Alternating Direction Methods, Numerische Math., Vol. 6, 1964, pp. 428-453.

11. Briley, W.R., Buggeln, R.C. and McDonald, H.: Computation of Laminar and Turbulent Flow in 90 Degree Square Duct and Pipe Bends Using the Navier-Stokes Equations, SRA Report R82-920009-F, 1982.

12. Eiseman, P.R.: Coordinate Generation with Precise Controls over Mesh Properties, J. of Comp. Physics, Vol. 47, 1982.

13. Thompson, J.F., Thames, F.C. and Mastin, C.W.: Automatic Numerical Generation of Body-Fitted Curvilinear Coordinate Systems for Fields Containing any Number of Artibrary Two-Dimensional Bodies, J. Comp. Physics, Vol. 15, 1974.

14. Oh, Y.H.: An Analytic Transformation Technique for Generating Uniformly Spaced Computational Mesh, Final Report, NASA-Langley Research Grant NSG1087, October 1978.

15. Briley, W.R. and McDonald, H.: Computation of Three-Dimensional Horseshoe Vortex Flow Using the Navier-Stokes Equations. Paper presented at Seventh International Conference on Numerical Methods in Fluid Dynamics, 1980.

16. Briley, W.R., McDonald, H. and Shamroth, S.J.: A Low Mach Number Euler Formulation and Application to Time Iterative LBI Schemes, AIAA Journal, Vol. 21, 1983.

17. Briley, W.R. and McDonald, H.: Computational Fluid Dyamic Aspects of Internal Flow, AIAA Paper 79-1455, 1979.

18. Yang, R.-J., Weinberg, B.C., Shamroth, S.J. and McDonald, H.: SRA Report 310003-10, 1984.

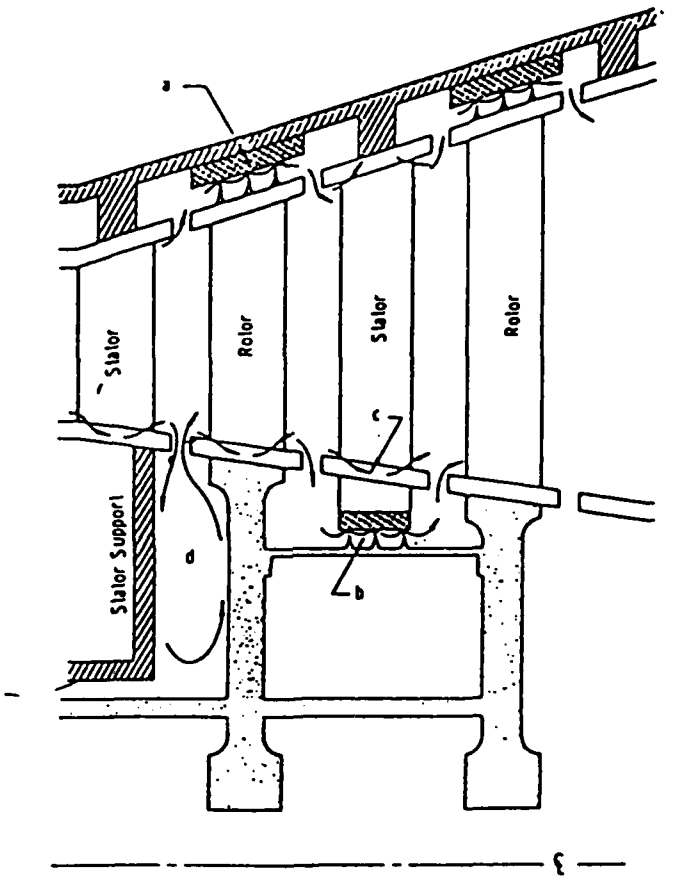

Fig. 1 - Disk Pumping Configuration

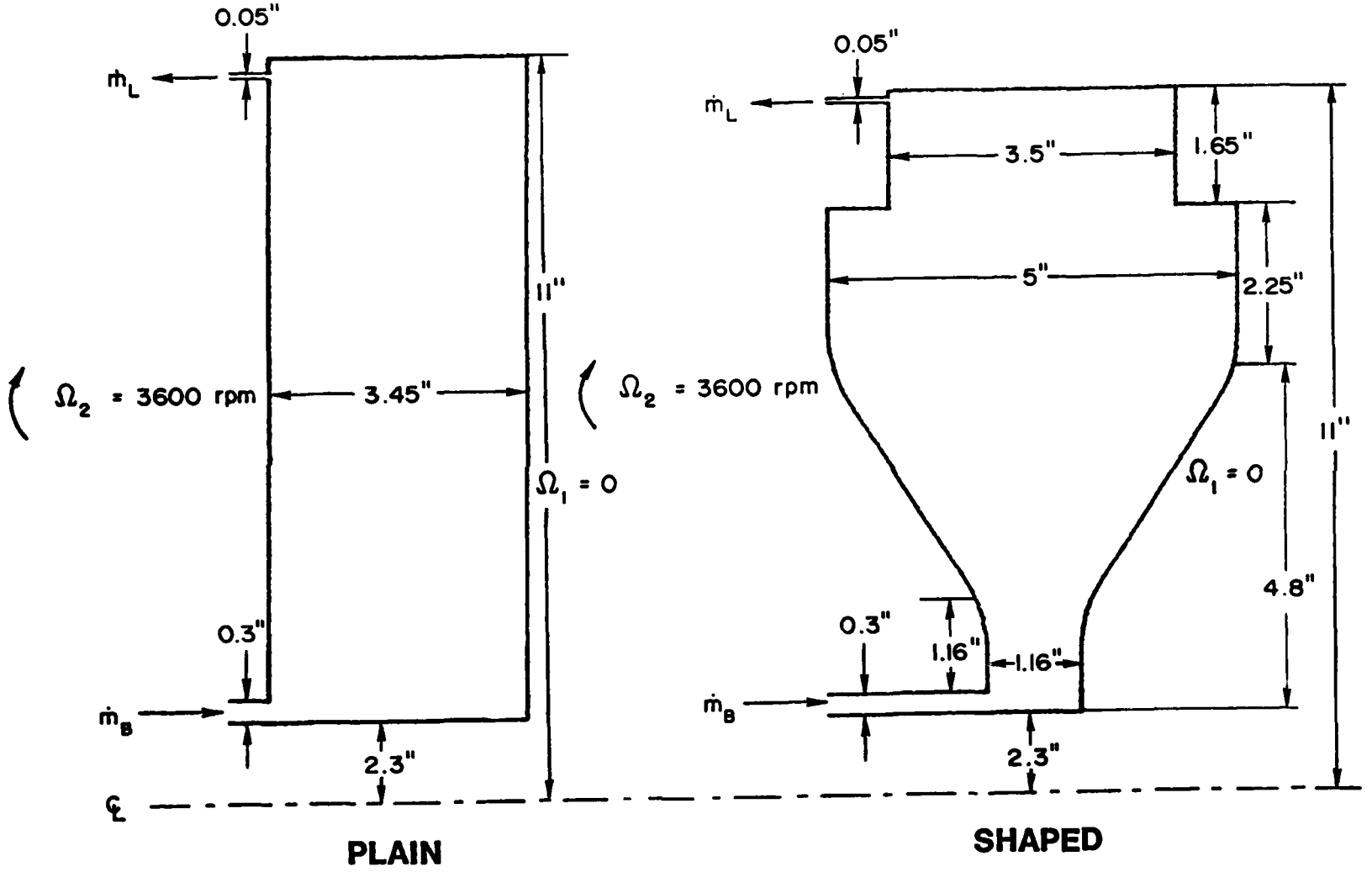

Fig. 2 - Schematic of Disk Configurations

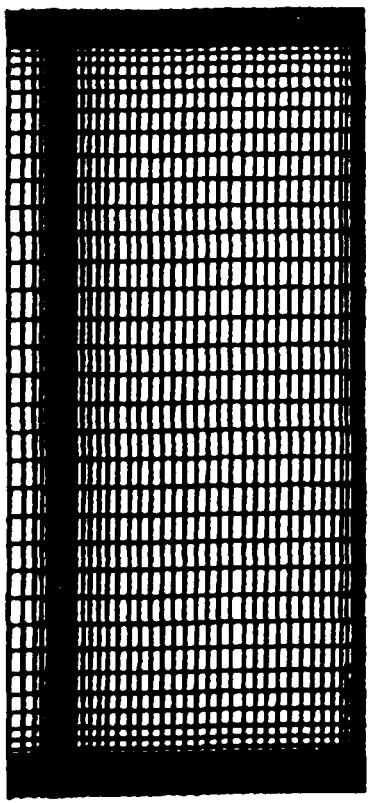

PLAIN

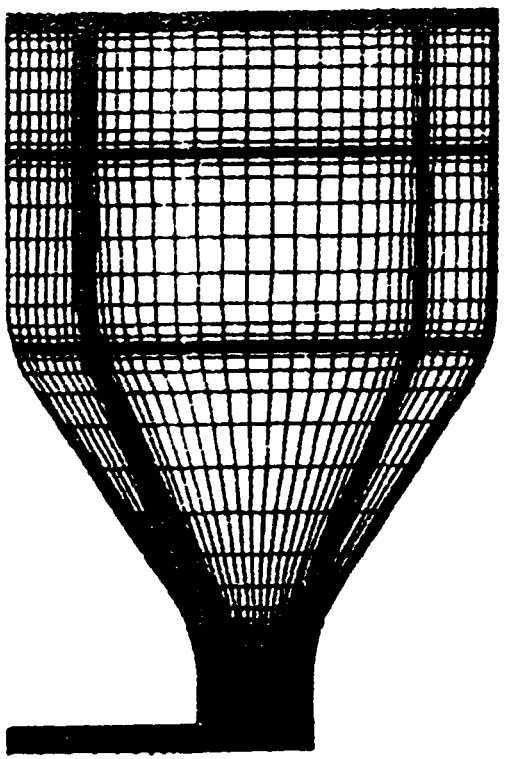

SHAPED

Fig. 3 - Coordinate Systems

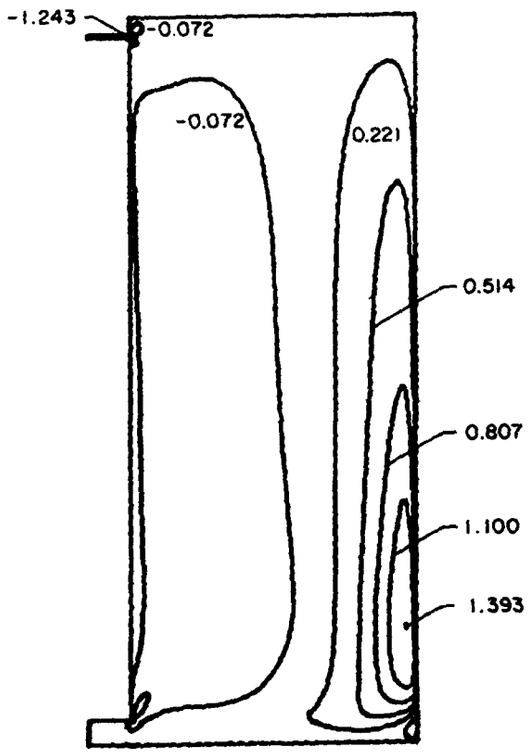

PLAIN

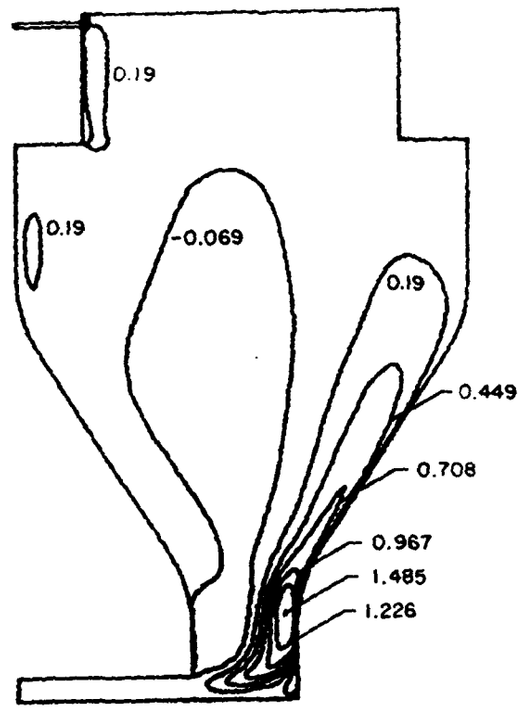

SHAPED

Fig. 4 - U-velocity Contours

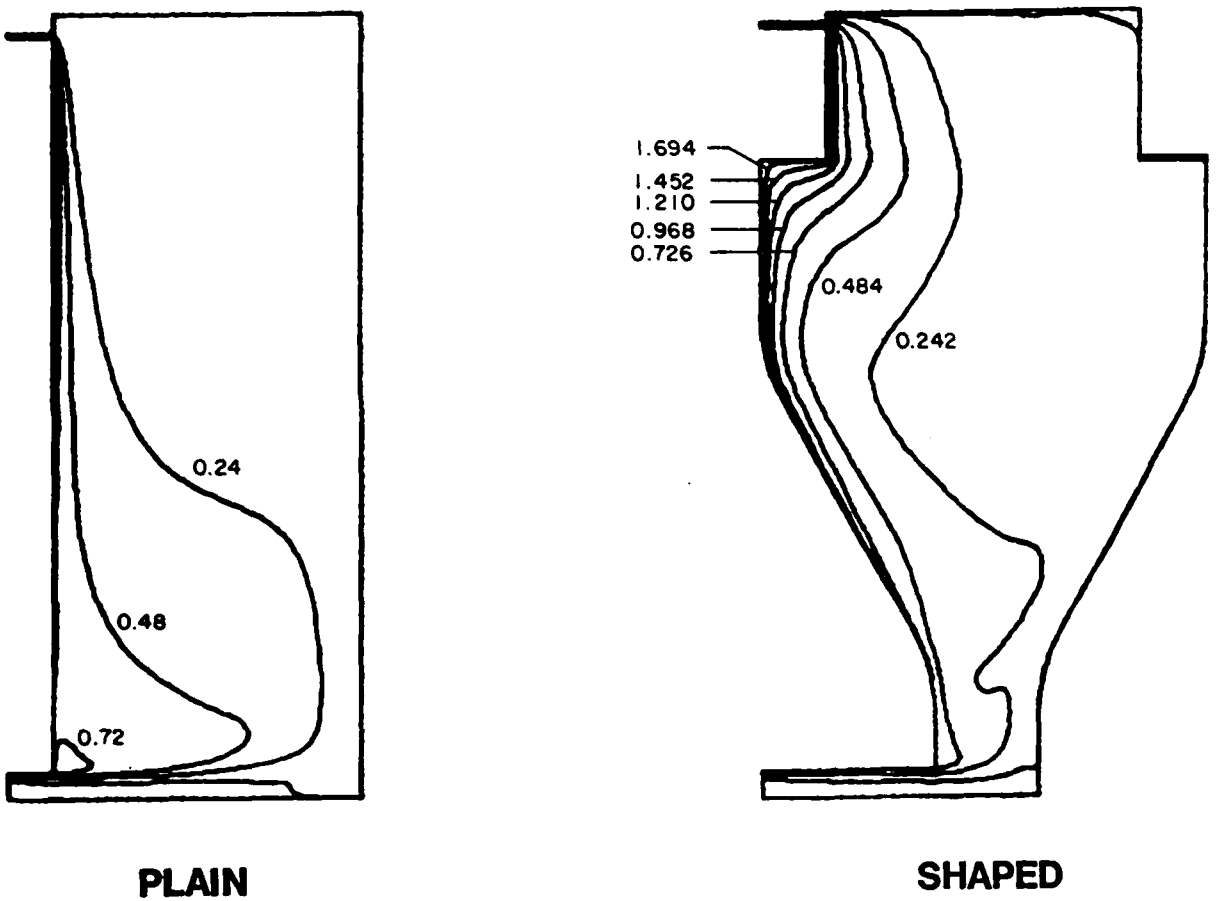

Fig. 5 - V-velocity Contours

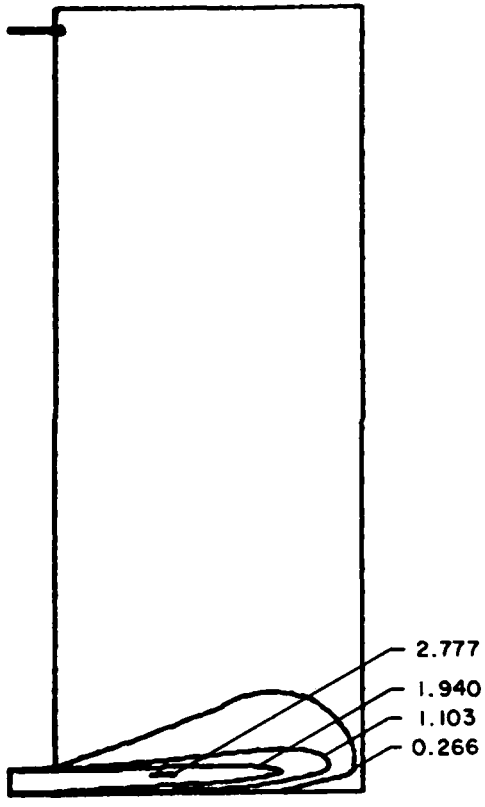

PLAIN

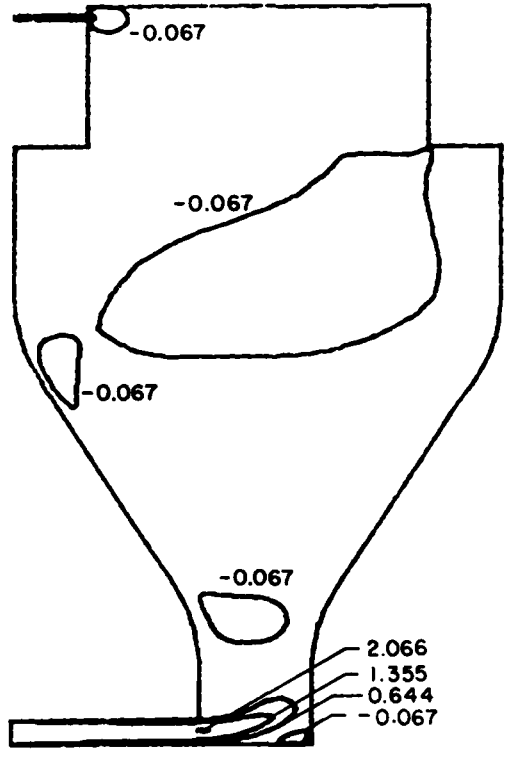

SHAPED

Fig. 6 - W-velocity Contours

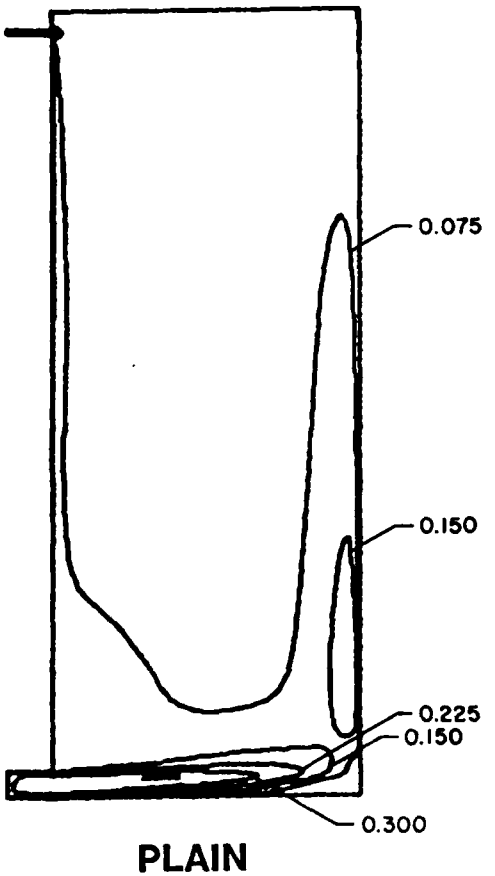

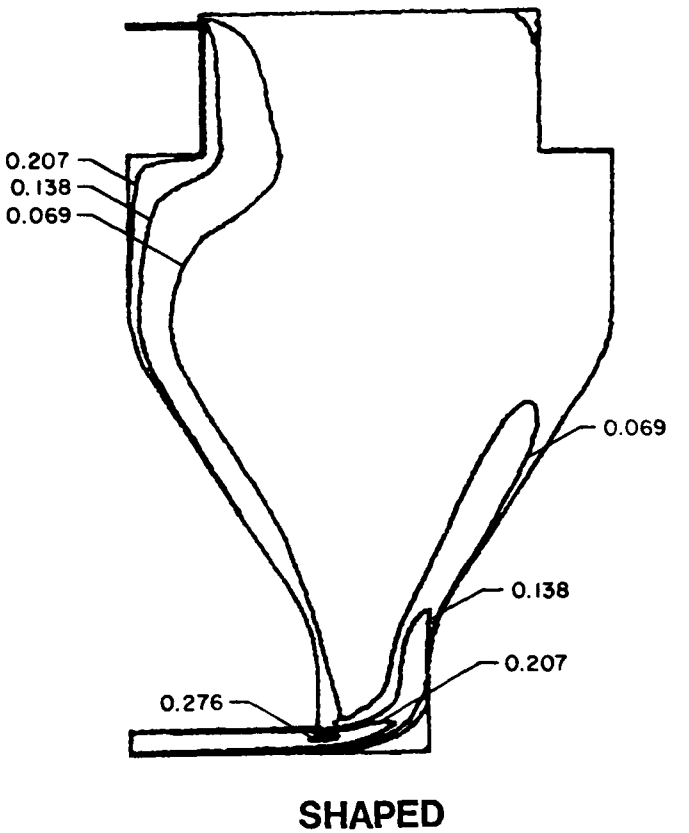

Fig. 7 - Mach No. Contours

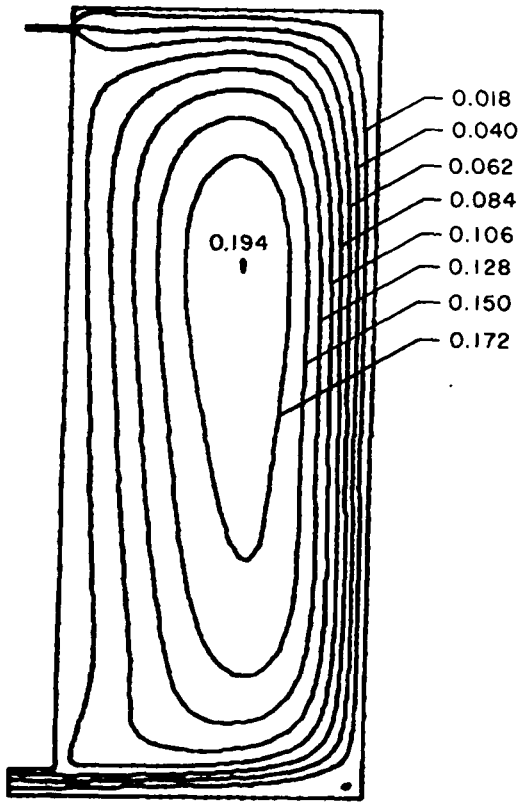

PLAIN

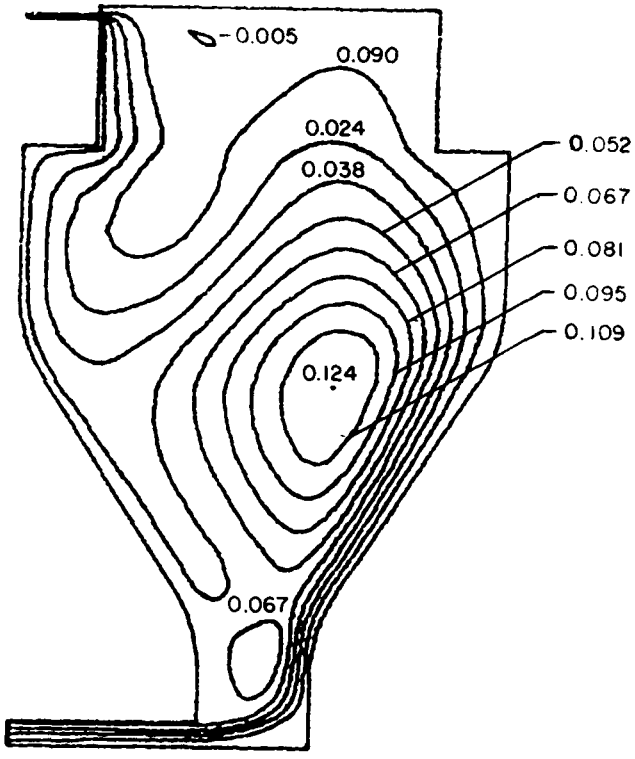

SHAPED

Fig. 8 - Stream Function

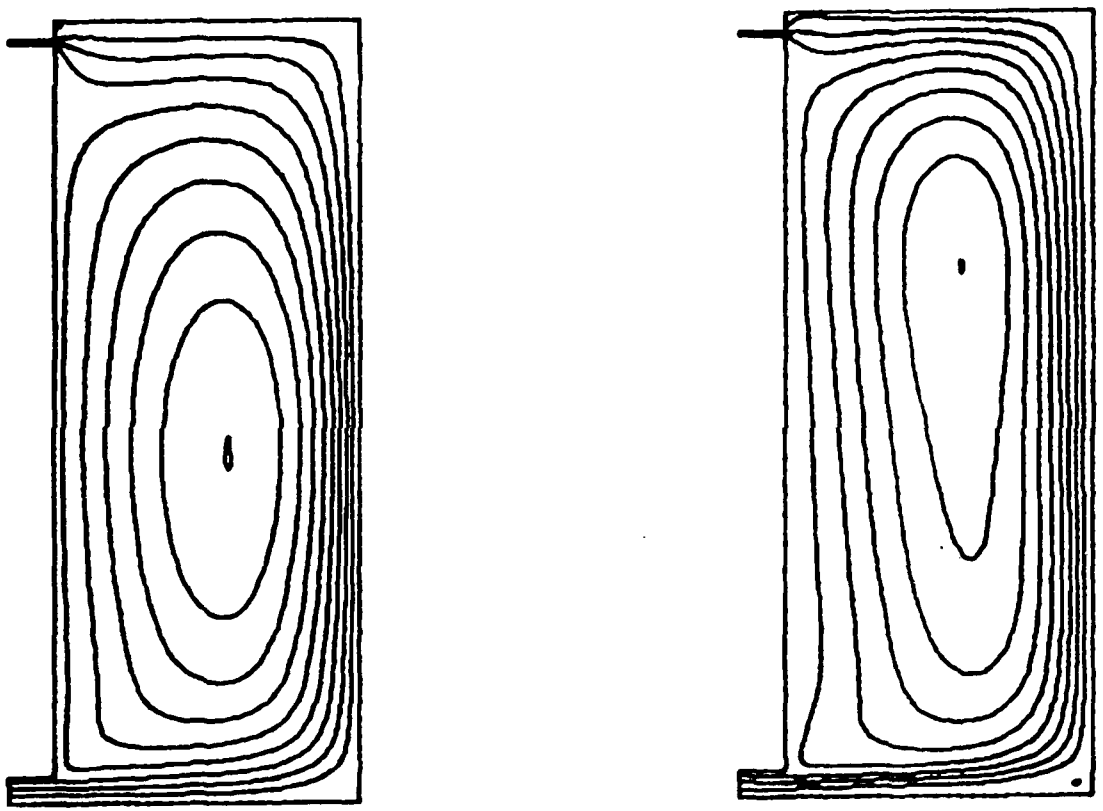

Fig. 9 - Effects of Rotation: Plain Disk Case

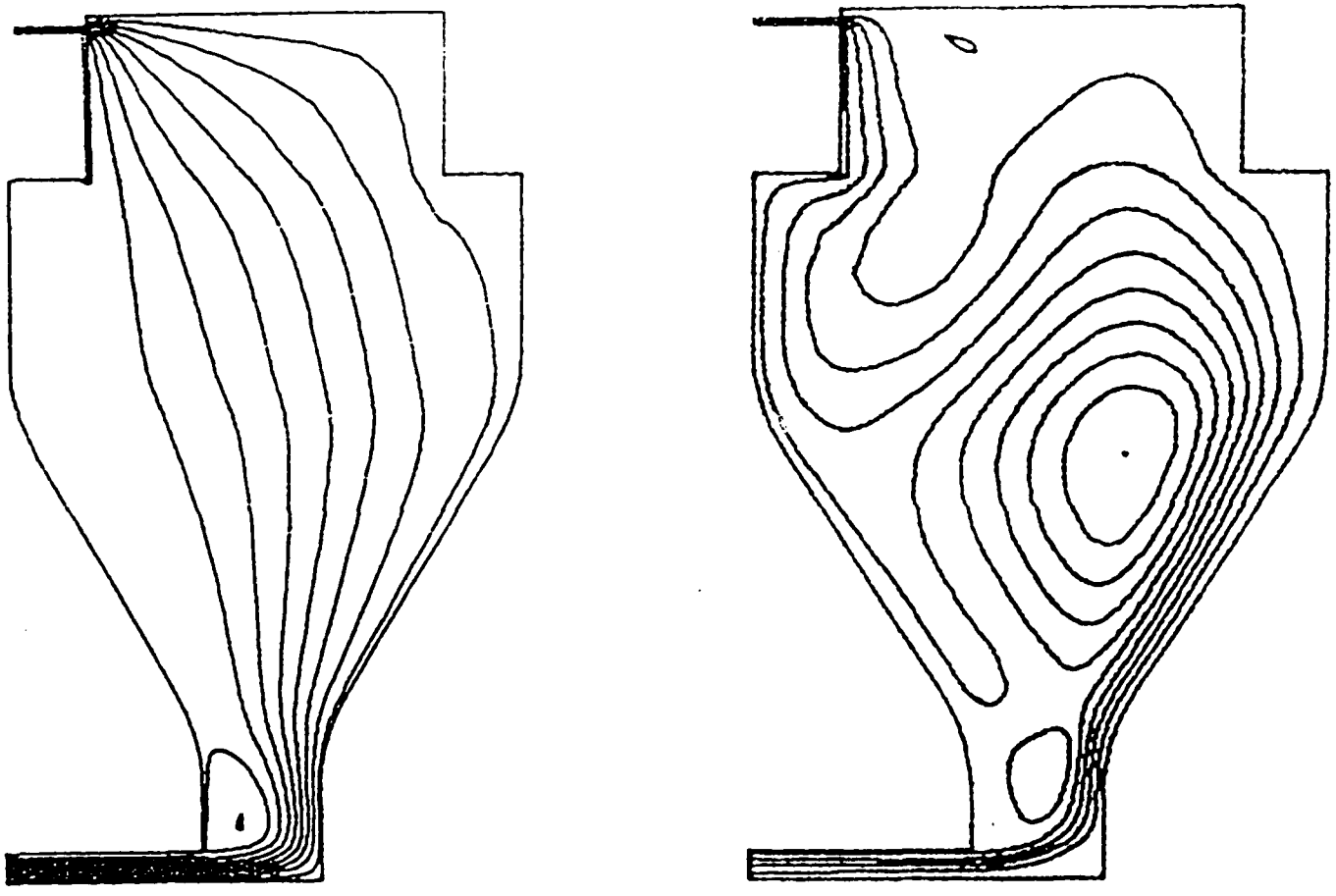

Fig. 10 - Effects of Rotation: Shaped Disk Case

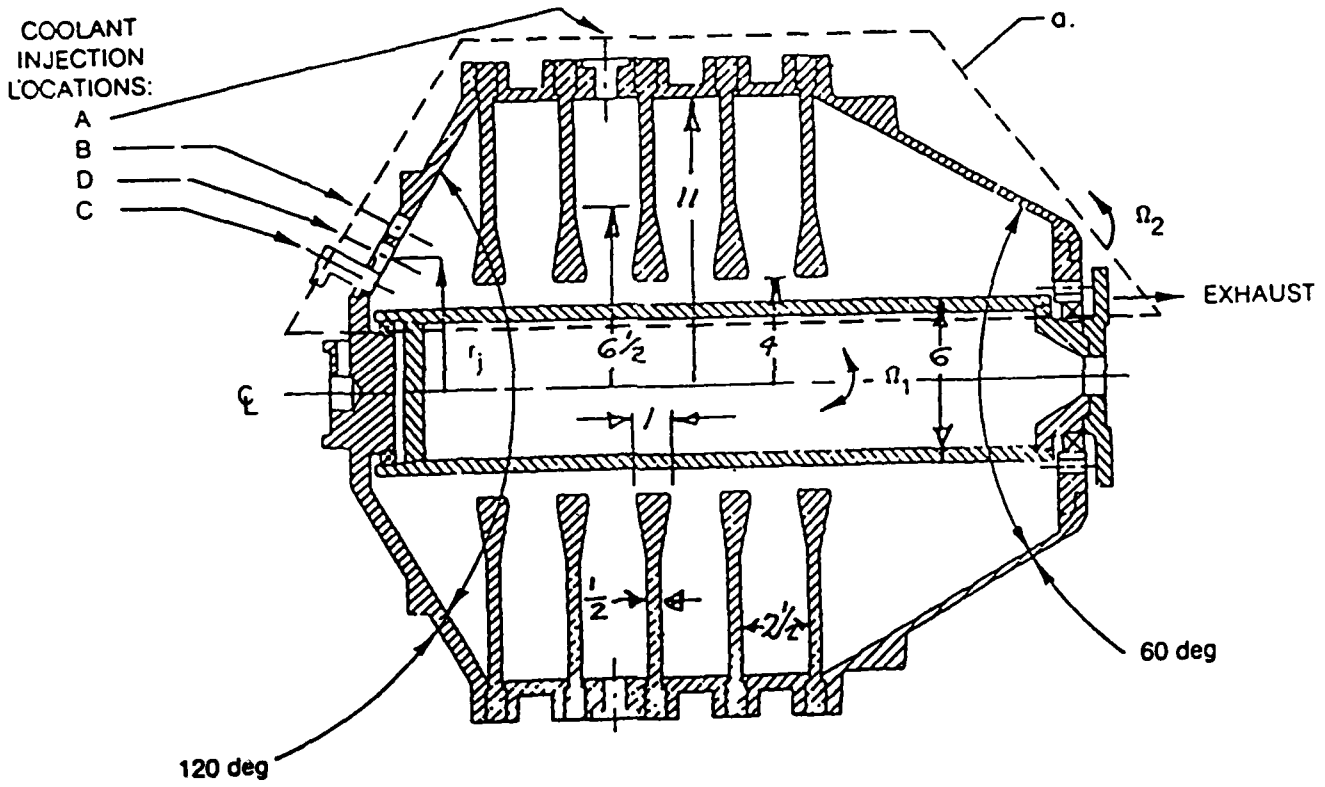

Fig. 11 - Sketch of Compressor Drum Model

APPENDIX A - Split LBI Algorithm

Linearization and Time Differencing

The system of governing equations to be solved consists of three/four equations: continuity and two/three components of momentum equation in three/four dependent variables: ρ, u, v, w. This system of equations can be written at a single grid point in the following form:

$$\partial H(\phi)/\partial t = D(\phi) + S(\phi) \qquad \text{(A-1)}$$

where ϕ is the column-vector of dependent variables, H and S are column-vector algebraic functions of ϕ, and D is a column vector whose elements are the spatial differential operators which generate all spatial derivatives appearing in the governing equation associated with that element.

The solution procedure is based on the following two-level implicit time-difference approximations of (Eq. 1):

$$(H^{n+1} - H^n)/\Delta t = \beta(D^{n+1} + S^{n+1}) + (1-\beta)\,(D^n + S^n) \qquad \text{(A-2)}$$

where, for example, H^{n+1} denotes $H(\phi^{n+1})$ and $\Delta t = t^{n+1} - t^n$. The parameter β ($0.5 \leq \beta \leq 1$) permits a variable time-centering of the scheme, with a truncation error of order $[\Delta t^2, (\beta - 1/2)\,\Delta t]$.

A local time linearization (Taylor expansion about ϕ^n) of requisite formal accuracy is introduced, and this serves to define a <u>linear</u> differential operator L such that

$$D^{n+1} = D^n + L^n(\phi^{n+1} - \phi^n) + O(\Delta t^2) \qquad \text{(A-3)}$$

Similarly,

$$H^{n+1} = H^n + (\partial H/\partial \phi)^n (\phi^{n+1} - \phi^n) + 0 (\Delta t^2) \qquad (A-4)$$

$$S^{n+1} = S^n + (\partial S/\partial \phi)^n (\phi^{n+1} - \phi^n) + 0 (\Delta t^2) \qquad (A-5)$$

Eqs. (3-5) are inserted into Eq. (2) to obtain the following system which is linear in ϕ^{n+1}

$$(A - \beta \Delta t\ L^n) (\phi^{n+1} - \phi^n) = \Delta t (D^n + S^n) \qquad (A-6)$$

and which is termed a linearized block implilcit (LBI) scheme. Here, A denotes a matrix defined by

$$A \equiv (\partial H/\partial \phi)^n - \beta \Delta t (\partial S/\partial \phi)^n \qquad (A-7)$$

Eq. (6) has 0 (Δt) accuracy unless $H \equiv \phi$, in which case the accuracy is the same as Eq. (2).

Special Treatment of Diffusive Terms

The time differencing of diffusive terms is modified to accomodate cross-derivative terms and also turbulent viscosity and artificial dissipation coefficients which depend on the solution variables. Although formal linearization of the convection and pressure gradient terms and the resulting implicit coupling of variables is critical to the stability and rapid convergence of the algorithm, this does not appear to be important for the turbulent viscosity and artificial dissipation coefficients. Since the relationship between μ_e and d_j and the mean flow variables is not conveniently linearized, these diffusive coefficients are evaluated explicitly at t^n during each time step. Notationally, this is equivalent to neglecting terms proportional to $\partial\ \mu_e/\partial\phi$ or $\partial d_j/\partial\phi$ in L^n, which are formally present in the Taylor series expansion (3), but retaining all terms proportional to μ_e or d_j in both L^n and D^n.

It has been found through extensive experience that this has little if any effect on the performance of the algorithm. This treatment also has the added benefit that the turbulence model equations can be decoupled from the system of mean flow equations by an appropriate matrix partitioning, and solved separately in each step of the ADI solution procedure. This reduces the block size of the block tridiagonal systems which must be solved in each step and thus reduces the computational labor.

In addition, the viscous terms in the present formulation include a number of cross-derivative terms implicitly within the ADI treatment which follows, it is not at all convenient to do so; and consequently, all cross-derivative terms are evaluated explicitly at t^n. For a scalar model equation representing combined convection and diffusion, it has been shown by Beam and Warming that the explicit treatment of cross-derivative terms does not degrade the unconditional stability of the present algorithm. To preserve notational simplicity, it is understood that all cross-derivative terms appearing in L^n are neglected but are retained in D^n. It is important to note that neglecting terms in L^n has no effect on steady solutions of Eq. (6), since $\phi^{n+1} \equiv 0$ and thus Eq. (6) reduces to the steady form of the equations: $D^n + S^n = 0$. Aside from stability considerations, the only effect of neglecting terms in L^n is to introduce an $0\ (\Delta t)$ truncation error.

Consistent Splitting of the LBI Scheme

To obtain an efficient algorithm, the linearized system (A-6) is split using ADI techniques. To obtain the split scheme, the multidimensional operator L is rewritten as the sum of three "one-dimensional" sub-operators L_i $(i = 1, 2, 3)$ each of which contains all terms having derivatives with respect to the i-th coordinate. The split form of Eq. (6) can be derived either as in (Refs. 4 and 5) by following the procedure described by Douglas and Gunn (Ref. 10) in their generalization and unification of scalar ADI schemes, or using approximate factorization. For the present system of equations, the split algorithm is given by

$$(A - \beta\Delta t L_1^n)\ (\phi^* - \phi^n) = \Delta t\ (D^n + S^n) \qquad \text{(A-8)}$$

$$(A - \beta\Delta t L_2^n)\ (\phi^{**} - \phi^n) = A\ (\phi^* - \phi^n) \qquad \text{(A-9)}$$

$$(A - \beta\Delta t L_3^n)\ (\phi^{n+1} - \phi^n) = A\ (\phi^{**} - \phi^n) \qquad \text{(A-10)}$$

where ϕ^* and ϕ^{**} are consistent intermediate solutions. If spatial derivatives appearing in L_i and D are replace by three-point difference formulas, as indicated previously, then each step in Eqs. (8-10) can be solved by a block-tridiagonal elimination.

U.S. GPO 559-065

END

FILMED

9-85

DTIC